Cellular Physiology and Biochemistry

Cell Physiol Biochem 2018;47:864-878
DOI: 10.1159/000490078
Published online: May 29, 2018
Accepted: April 11, 2018

Original Paper

Exosomes from MiR-30d-5p-ADSCs Reverse Acute Ischemic Stroke-Induced, Autophagy-Mediated Brain Injury by Promoting M2 Microglial/Macrophage Polarization

Mei Jiang[a] Hairong Wang[b] Mingming Jin[c] Xuelian Yang[a] Haifeng Ji[a] Yufeng Jiang[d] Hanwen Zhang[a] Feifei Wu[a] Guolu Wu[a] Xiaoyin Lai[a] Liying Cai[a] Rongguo Hu[a] Limin Xu[c] Longxuan Li[a]

[a]Department of Neurology, Shanghai Gongli Hospital, The Second Military Medical University, Shanghai, [b]Department of Cardiology, Shanghai Gongli Hospital, The Second Military Medical University, Shanghai, [c]Department of Central Laboratory, Shanghai Gongli Hospital, The Second Military Medical University, Shanghai, [d]Department of Clinical Medicine, Clinical Medical School of Anhui Medical University, Anhui, P.R. China

Key Words
Acute ischemic stroke • MiR-30d-5p • Microglial/macrophage polarization • Autophagy • Exosome

Abstract
Background/Aims: Recent studies have indicated that exosomes secreted from adipose-derived stem cells (ADSCs) have important effects in the treatment of ischemic injury. However, the treatment mechanism is unclear. This study aimed to investigate whether ADSC-derived exosomes enriched with microRNA (miR)-30d-5p have a protective effect on acute ischemic stroke (AIS). ***Methods:*** In the current study, inflammatory factors and miR-30d-5p expression were assessed in 70 subjects with AIS and 35 healthy controls. Exosomes were characterized by transmission electron microscopy and further examined using nanoparticle tracking analyses. A rat model of AIS and an *in vitro* model of oxygen- and glucose-deprived (OGD) primary microglia were established to study the protective mechanism of exosomes from miR-30d-5p-overexpressing ADSCs in ischemia-induced nerve injury. ***Results:*** The results showed that following AIS, the expression of inflammatory cytokines increased, while the anti-inflammatory cytokines IL-4, IL-10, and miR-30d-5p decreased both in patients and in animal models. Moreover, *in vitro* studies demonstrated that suppression of autophagy significantly reduced the OGD-induced inflammatory response. In addition, exosome treatment was more effective in suppressing the inflammatory response by reversing OGD-induced and

M. Jiang, H. Wang and M. Jin contributed equally to this work.

Longxuan Li
and Limin Xu

Department of Neurology, Shanghai Gongli Hospital, Second Military Medical University 219 Miao-Pu Road, Shanghai 200135 (China)
Tel. +86-021-58858730, E-Mail Longxuanlee2006@yahoo.com, 13564378807@163.com

autophagy-mediated microglial polarization to M1. Furthermore, *in vivo* studies showed that exosomes derived from ADSCs significantly decreased the cerebral injury area of infarction by suppressing autophagy and promoting M2 microglia/macrophage polarization. ***Conclusions:*** Our results suggest that miR-30d-5p-enhanced ADSC-derived exosomes prevent cerebral injury by inhibiting autophagy-mediated microglial polarization to M1.

Introduction

Stroke is one of the leading causes of death worldwide and results in disabilities in approximately 75% of its survivors [1, 2]. Increasing evidence has shown that the changed microenvironment in cerebral tissue plays an important role in cerebral injury after ischemia, particularly the inflammatory response [3]. Microglial activation and promotion of M1 microglial/macrophage polarization play central roles in neuroinflammation after brain injury [4, 5]. Microglia/macrophages are known to have different phenotypes with distinct functions during the course of ischemic brain injury [5]. M2 microglia protect neighboring cells by removing cell debris and releasing trophic factors for brain repair, based on their ability to produce interleukin 4 (IL-4) and IL-10 [6]. Meanwhile chronically-activated M1 microglia exacerbate brain injury by producing neurotoxic substances, although they participate in clearing cell debris in the early stages after stroke [7]. Microglia/macrophage phenotype polarization is likely dependent on activation status, and balancing this polarization is a promising therapeutic strategy for stroke treatment.

Autophagy is a homeostatic process that can prevent damage to healthy cells [8]. Autophagy not only contributes to human physiological events, but also can paradoxically cause some pathological conditions [9]. Recently, there has been increased evidence that autophagic dysfunction could be implicated in the development of neuro-degenerative diseases, cancer, infection and diseases of aging [10, 11]. However, it is unclear whether autophagy acts primarily on the inflammatory response relative to microglia/macrophage polarization.

MicroRNAs (miRNAs), a family of non-coding RNAs of 20–25 nucleotides, play pivotal roles during this remodeling process by regulating target genes at the post-transcriptional level [12, 13]. Several studies have demonstrated significant alterations in the cerebral "miRNA-ome" following ischemia [14, 15]. These reports suggest that miRNAs may act as innovative gene therapeutic candidates contributing to neurogenesis, angiogenesis, and neural plasticity [16, 17]. A clinical study found that miR-30d-5p was downregulated in the brain cortex after hypoxia-ischemia and this miRNA is known to play an important role in regulation of autophagy and apoptosis in developing rat brains after hypoxic-ischemic injury [18]. Bioinformatics analysis (http://www.targetscan.org/) found that the expression of miR-30d-5p can target Beclin-1 and Atg5, suggesting that the expression of miR-30d-5p may play an important role in suppression of autophagy.

Mesenchymal stromal cells (MSCs) have been extensively investigated for their therapeutic properties after ischemic injury via paracrine/endocrine mechanisms [19, 20]. Exosomes (Exos) derived from MSCs have been described as a novel pathway of cell-to-cell interaction and a crucial point in signal regulation [21-23]. These membranous structures which deliver exogenous functional mRNA and miRNA sequences to target cells contribute to disease progression and can help to treat diseases. However, few studies of Exos have focused on their miRNA regulatory function in acute ischemic stroke (AIS). In the current study, we evaluated the therapeutic effect of exosomes secreted by adipose-derived stem cells (ADSCs) overexpressing miR-30d-5p on the ischemia-induced cerebral injury in AIS rats.

Materials and Methods

Clinical specimen collection and ethics statement

All patients were diagnosed as having an AIS according to the World Health Organization criteria [24]; all presented with their first episode of cerebral infarction and received treatment within 48 hours after hospitalization in the Department of Neurology of the Pudong New Area Gongli Hospital. The control group was selected from 30 patients without acute cerebral infarction. Patients with the following conditions were excluded from both groups of the present study: liver/kidney dysfunction, heart failure, severe infection, malignant disease, symptoms of potential infection in the past 4 weeks, and surgical or trauma history, or consumption of aspirin, lipid-lowering drugs (statin), or antihypertensive drugs (angiotensin converting enzyme inhibitors) within the last 2 weeks. Peripheral blood samples were obtained from 70 patients with AIS and 35 healthy volunteers (Table 1). Expression of the inflammatory factors inducible nitric oxide synthase (iNOS), IL-6, IL-1β, IL-4, IL-10 and tumor necrosis factor (TNF)-α in serum were measured using commercially-available ELISA kits (Sen-Xiong Company, Shanghai, China). The expression of miR-30d-5p in serum was detected by real-time polymerase chain reaction (RT-PCR). The study was approved by the ethics committee of Pudong New Area Gongli Hospital. All participants or their relatives were informed of the study and signed the consent forms before inclusion in the study.

Table 1. Clinicopathological characteristics of AIS patients and healthy controls. AIS, acute ischemic stroke; BMI, body mass index; NIHSS, National Institutes of Health Stroke Scale; CHD, coronary heart disease; WBC, white blood cells; RBC, red blood cells; Hb, hemoglobin; PLT, platelets; ESR, erythrocyte sedimentation rate; TC, Total cholesterol; TG, Triglycerides; HDL, High-density lipoproteins; LDL, Low-density lipoproteins; AI, atherogenic index. Data are presented as mean ± standard. *P < 0.05, ***P < 0.001 vs healthy controls

Characteristics	Controls (35)	AIS (70)
Age (years)	69.7 ± 12.0	68.2 ± 12.8
Sex		
Male	18	40
Female	17	30
Weight (kg)	79.6 ± 11.3	80.5 ± 13.2
Height (m)	1.69 ± 0.1	1.71 ± 0.1
BMI	27.1 ± 2.9	27.2 ± 3.1
NIHSS	-	12.8 ± 2.6
Risk factors (no)		
Hypertension, n (%)	-	49 (70.0%)
CHD, n (%)	-	21 (30.0%)
Laboratory findings		
WBC (109/L)	5.9 ± 1.8	10.6 ± 6.5***
RBC (1012/L)	4.7 ± 0.4	4.8 ± 0.5
Hb (g/L)	143.3 ± 11.3	146.4 ± 12.1
PLT (109/L)	244.2 ± 71.8	249.3 ± 65.5
ESR (mm/h)	5.3 ± 1.8	18.7 ± 4.3***
TC (mmol/L)	5.1 ± 0.5	4.9 ± 0.4
TG (mmol/L)	1.3 ± 0.18	1.4 ± 0.17
HDL (mmol/L)	1.0 ± 0.11	1.03 ± 0.07
LDL (mmol/L)	2.91 ± 0.72	2.98 ± 0.85
AI	2.6 ± 0.4	3.4 ± 0.4*

Animals and ethics statement

Male Sprague–Dawley rats (230–280 g) were purchased from Shanghai Sippr Bk Laboratory Animals Co. Ltd. (Shanghai, China). All rats were allowed free access to food and water under controlled conditions (12/12 h light/dark cycle with humidity of 60 ± 5%, and a temperature of 22 ± 3 °C). All animals were treated in accordance with the Guide for the Care and Use of Laboratory Animals, and all experiments were approved and performed according to the guidelines of the Ethics Committee of Pudong New Area Gongli Hospital, Shanghai, China. All surgical procedures were performed under anesthesia, and every effort was made to minimize suffering. Rats were anesthetized by intraperitoneal injection of sodium pentobarbital (30 mg/kg).

Microglia isolation and culture

Neonatal rats were anesthetized, fully disinfected with 75% alcohol under anesthesia, then placed on ice and decapitated. The whole brain was dissected to obtain mixed glia cells. The meninges and blood vessels were removed carefully using ophthalmic forceps, then brain tissues were minced using ophthalmic scissors, and enzymatically digested using 0.125% trypsin at 37 °C for 60 min. Samples were separated by centrifugation at 1, 200 × *g* for 10 min and filtered through a 70 μm cell strainer. The mixed cells were cultured in 25 cm^2 flasks which had been coated with poly-L-lysine (PLL). Each flask contained 6 mL DMEM/F12 medium (Gibco, Thermo Fisher Scientific, Waltham, MA, USA) containing 10% FBS (Gibco) and 1% Pen/Strep (Solarbio, Beijing, China). Cell concentration was approximately 10^6 cells/mL calculated using a hemocytometer. The cells were cultured in a constant-temperature incubator (Sanyo, Osaka, Japan) containing 5% CO_2 at 37 °C. After culture for 7–9 days, microglia were isolated from the mixed glia by gentle shaking [25].

Transfection of cells with the miR-30d-5p mimic vector

For miR-30d-5p overexpression, the miR-30d-5p mimic or corresponding negative control (miR-NC) were purchased from GenePharma (Shanghai, China). ADSCs were transfected with either the miR-30d-5p mimic or miR-NC at a final concentration of 50 nM using Lipofectamine® 2000 (Invitrogen, Carlsbad, CA, USA) according to the manufacturer's protocol. Cells were used for miR-30d-5p expression analysis or other experiments after 48 h of transfection.

RNA and miRNA extraction and real-time polymerase chain reaction

Total RNA was isolated from serum or cells using Trizol reagent. First strand cDNA was synthesized using the PrimeScript™ RT Master Mix (Perfect Real Time) Kit (RR036A, Takara Bio Inc., Shiga, Japan), which was then used for RT-PCR, together with forward and reverse primers and the Power SYBR Green PCR Master Mix (Life Technologies, Thermo Fisher Scientific). U6 was used as the internal control. The primer sequences were: U6 (sense 5'-GCTTCGGCAGCACATATACTAAAAT-3', antisense 5'-CGCTTCACGAATTTGCGTGTCAT-3') and miR-30d-5p (sense 5'-GCCTGTAAACATCCCCGAC-3', antisense 5'-GTGCGTGTCGTGGAGTCG-3'). Quantification of miR-30d-5p and endogenous control mRNA U6 were performed using TaqMan assays. Data were analyzed using the $2^{-\Delta\Delta Ct}$ method.

Enzyme-linked immunosorbent assay (ELISA)

The inflammatory factors iNOS, IL-6, IL-1β, IL-4, IL-10 and TNF-α in serum or cell supernatant were measured using a commercially-available ELISA kit (Sigma-Aldrich, St Louis, MO, USA). All procedures were performed according to the manufacturer's instructions.

ADSCs isolation and characterization

Adipose tissue was harvested from normal SD rat. Then, the tissue was washed with phosphate-buffered saline (PBS) and mechanically chopped before digestion with 0.2% collagenase I (Sigma) for 1 h at 37 °C with intermittent shaking. The digested tissue was washed with Dulbecco's modified Eagle's medium (DMEM) (Sigma) containing 15% fetal bovine serum (FBS), and then centrifuged at 1000 rpm for 10 min to remove mature adipocytes. The cell pellet was resuspended in DMEM supplemented with 15% FBS, 100 U/ml penicillin, and 100 μg/ml streptomycin in a 37°C incubator with 5% CO_2. ADSCs reaching 80%–90% confluency were detached with 0.02% ethylenediaminetetaacetic acid (EDTA)/0.25% trypsin (Sigma-Aldrich) for 5 min at room temperature and then replated. For phenotypic analysis, fluorescein isothiocyanate (FITC-F) or phycoerythrin (PE) were used. The expression of the following markers was investigated: CD29, CD90, CD44, CD105, and vWF. An IgG-matched isotype served as the internal control for each antibody. For normoxic cultures, ADSCs were cultured in 95% air (20% O_2) and 5% CO_2.

Exosome isolation and characterization

Exosomes were purified from the cell culture supernatant of ADSCs (ADs-Exos). Prior to collection of culture medium, ADSCs were washed twice with phosphate-buffered saline (PBS), and the medium was changed to serum-free medium. After incubation for 48 h, the supernatant was collected and treated by sequential ultracentrifugation at 2, 000 × *g* for 30 min, 10, 000 × *g* for 30 min, and 100, 000 × *g* for 4 h at 4 °C. To avoid contamination with FBS-derived exosomes, exosome-free FBS (Gibco) was used to culture ADSCs. The isolated exosomes were washed once with PBS and resuspended for further characterization.

To analyze the size distribution of ADs-Exos, Nanosizer™ technology (Malvern Instruments, Malvern, UK) was adopted. For transmission electron microscopy (TEM), purified exosomes from ADSCs were resuspended in PBS and imaged as detailed previously [26]. The proteins encapsulated into exosomes were analyzed by classical western blotting to test for the specific exosome markers CD9, CD63, CD81, and TSC101

Exosome labeling and uptake

Exosomes were labeled with a DiI fluorescent labeling kit (Sigma-Aldrich). DiI (400 μL) was added to the exosome suspension and incubated for 5 min at room temperature. The reaction was stopped by the addition of an equal volume of exosome-depleted bovine serum albumin and then the exosomes were washed twice with PBS to remove any unbound dye. Subsequently, the DiI-labeled or denatured exosomes were incubated with primary microglia for 24 h or sacrificed 3 h after intravenous injection through the tail vein into ischemic rats. The cells or brain slices were then fixed and stained with 4',6-diamidino-2-phenylindole (DAPI). The images were obtained under a confocal microscope.

Oxygen and glucose deprivation (OGD) treatment

Combined oxygen and glucose deprivation was performed as described previously [27]. Briefly, ischemia was induced by changing the cells into an ischemia-mimetic solution–Hanks' solution (140 mM NaCl, 3.5 mM KCl, 0.43 mM KH_2PO_4, 1.25 mM $MgSO_4$, 1.7 mM $CaCl_2$, 5 mM $NaHCO_3$, 20 mM HEPES, pH 7.2–7.4) and placing the culture dishes in a hypoxic incubator chamber (Billups-Rothenberg, San Diego, CA, USA) equilibrated with 95% N_2/5% CO_2 at 37 °C for 6 h. The buffered Hanks' solution was previously gassed with 95% N_2/5% CO_2 for 30 min. The exosome treatment groups were treated with 10 μg/mL exosomes from ADSCs or miR-30d-5p added into the Hanks' solution. The 3-methyladenine (3-Ma) treatment group was treated with 2 mM 3-Ma in Hanks' solution. Control cells incubated in DMEM/F12 were run in parallel for each condition for the corresponding period of time.

Immunofluorescence

Cells or tissues were incubated with LC-3, Iba-1, CD206, iNOS antibodies or TUNEL (InvivoGen, San Diego, CA, USA) overnight at 4 °C, then incubated with conjugated secondary antibody for 1 h at room temperature in the dark. After several washes with PBS, the slides were incubated with DAPI for 3 min and then mounted in glycerol. The fluorescence was assessed under a fluorescence microscope.

Luciferase reporter assay

To construct luciferase reporter vectors, the 3'-UTR of Atg5 and Beclin-1 cDNA fragments containing the predicted potential miR-30d-5p binding sites were amplified by PCR and subcloned downstream of the luciferase gene in the PYr-MirTarget luciferase vector (Ambion, Austin, TX, USA). The 3'-UTR of Atg5 and Beclin-1 (containing the binding sites for miR-30d-5p) were amplified from a cDNA library with the following primers: Atg-5 (forward, 5'-CTCGAGCC*TTAATGAGAATTTCCTGTTTACA*GTC-3' and reverse, 5'-GCGGCCGCGAACTCCTGAGACGAGTTCCCC-3'); Beclin-1 (forward, 5'-CTCGAGGG*TAATATTAAACCACATGTTTACAA*TAC-3' and reverse, 5'-GCGGCCGCCCAGTGAAAACACATTAATGTC-3'). The mutant 3'-UTR of Beclin-1 and Atg5 (in which six nucleotides were mutated in the binding sites) were amplified using the following primer sequences: Atg-5 (forward, 5'-CTCGAGCC*TTAATGAGAATTTCCTCAATGAA*GTC-3' and reverse, 5'-GCGGCCGCGAACTCCTGAGACGAGTTCCCC-3'); Beclin-1 (forward, 5'-CTCGAGGG*TAATATTAAACCACATCAATGAAA*TAC-3' and reverse, 5'-GCGGCCGCCCAGTGAAAACACATTAATGTC-3').

For luciferase assays, HEK293T cells were cultured in 24-well plates and co-transfected with 50 ng of the corresponding vectors containing firefly luciferase together with 25 ng of miR-30d-5p or control. Transfection was performed using Lipofectamine® 2000 reagent (Invitrogen). At 48 h post-transfection, the relative luciferase activity was calculated by normalizing the firefly luminescence to the Renilla luminescence using the Dual-Luciferase Reporter Assay (Promega, Madison, WI, USA) according to the manufacturer's instructions.

Murine models of middle cerebral artery occlusion (MCAO)

Animals were anesthetized by intraperitoneal injection of pentobarbital sodium. Body temperature was monitored and maintained at 36.5 to 37.5 °C. A modified model of MCAO was used to create permanent focal ischemia, as previously described [26] . Briefly, the right middle cerebral artery (MCA) was occluded by inserting a monofilament nylon suture with a heat-rounded tip into the internal carotid artery, which was advanced further until it closed the origin of the MCA. Sham-operated rats underwent the same surgical procedure without insertion of the filament. To investigate the effect of exosomes from ADSCs on MCAO-induced cerebral injury, DiI-labeled exosomes (DiI-Exos) were resuspended in 0.9% saline and injected intravenously through the tail vein into ischemic rats at a concentration of 80 μg per 2 ml immediately after the ligation operation [28]. Rats were sacrificed 3 h or 72 h after injection and the brain sections were harvested.

Western blot analysis

Western blot analysis was carried out using cell lysates in urea buffer (8 M urea, 1 M thiourea, 0.5% 3-[(3-cholamidopropyl) dimethylammonio]-1-propanesulfonate (CHAPS), 50 mM dithiothreitol, 24 mM spermine). Protein fractions were prepared using extraction reagents (Pierce, Rockford, IL, USA) following

the manufacturer's protocols. GAPDH was used as the loading control. Samples (40 μg total protein) were separated by sodium dodecyl sulfate polyacrylamide gel electrophoresis (SDS-PAGE) and transferred to nitrocellulose membranes (Merck-Millipore, Darmstadt, Germany). After blocking in 5% nonfat milk for 1 h, the membranes were incubated with primary antibodies against Beclin-1 (1:1000), P62 (1:200), LC3 (1:200), Atg5 (1:200) or GAPDH (1:2000) at 4 °C overnight. After washing, the membranes were incubated with horseradish peroxidase-conjugated secondary antibodies for 1 h at room temperature. Signals were detected using an ECL detection system (GE Healthcare, Aurora, OH, USA) and analyzed using ImageJ 1.42q software (National Institutes of Health, Bethesda, MD, USA)

Statistical analysis

Results are expressed as the mean ± standard deviation (SD). Statistical significance was evaluated by analysis of variance followed by the Tukey–Kramer multiple comparison test and Student's *t*-test. $P < 0.05$ denotes statistical significance.

Results

The expression of miR-30d-5p and inflammatory factor in serum were different in stroke patients

The obtained data demonstrate that AIS did not alter blood Hb, RBC or PLT count, whereas a significant 70.5% increase in WBC count was observed in patients after AIS compared to the control values (Table 1). In addition, ESR in AIS exceeded control levels by more than 3-fold. No significant differences in serum TC, TG, HDL or LDL were detected between the studied groups. RT-PCR detection showed that the expression of miR-30d-5p was down-regulated after AIS (Fig. 1A). The result was consistent with the findings of Zhao, *et al* [18].. In addition, there is increasing evidence that the expression of miR-30d-5p is related to autophagy regulation [18] and inflammatory response [29]. ELISA detection showed that serum levels of the inflammatory factors TNF-α, IL-6 and iNOS were upregulated in AIS patients, while the anti-inflammatory factors IL-4 and IL-10 were down-regulated (Fig. 1B-F). According to previous reports, TNF-α, IL-6 and iNOS might be involved in the inflammatory responses in acute cerebral infarction patients and are also M1 macrophage markers, while IL-4 and IL-10 are M2 macrophage markers [30]. Together the above results show that the M1 macrophage polarization of microglial cells is enhanced after AIS which promotes the inflammatory response. These findings suggest that expression of miR-30d-5p may be involved in inflammatory factor regulation.

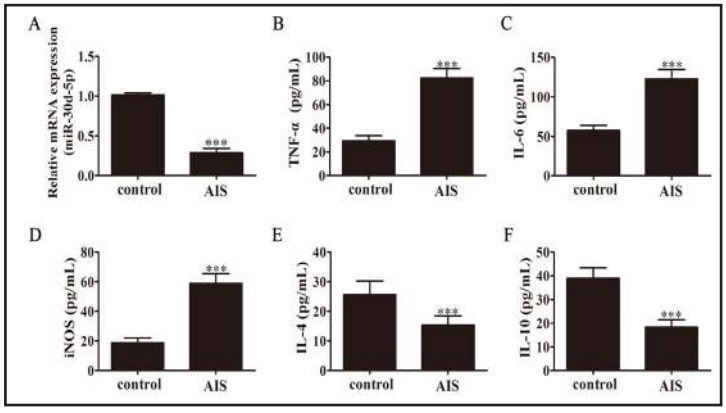

Fig. 1. The expression of miR-30d-5p and inflammatory factors in stroke patients. (A) The expression of miR-30d-5p in serum from stroke patients or healthy controls was measured by RT-PCR. Data are presented as mean ± SD. ***P<0.001 vs. control group. (B–F) ELISA analysis shows the expression levels of TNF-α (B), IL-6 (C), iNOS (D), IL-4 (E) and IL-10 (F). Data are presented as mean ± SD. ***P<0.001 vs. control group.

Exos from miR-30d-5p-overexpressing ADSCs are more effective in suppressing OGD-induced autophagy in primary microglia

There is increasing evidence that autophagy has a regulatory function in inflammation as well as having an anti-inflammatory effect [31, 32]. However some reports found that autophagy might

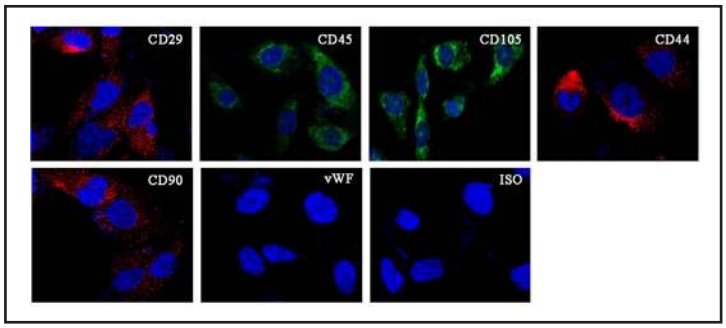

Fig. 2. Characteristics of adipose-derived stem cells (ADSCs). Determination of cell surface markers with immunofluorescence staining. The antibodies were labeled either with fluorescein isothiocyanate (FITC; green color) or with phycoerythrin (PE; red color), respectively. CD29, CD90, CD44, CD45 and CD105 stained positive. von Willebrand Factor (vWF) staining are negative. Negative FITC and PE labeled mouse IgG isotype controls are shown (magnification, ×200).

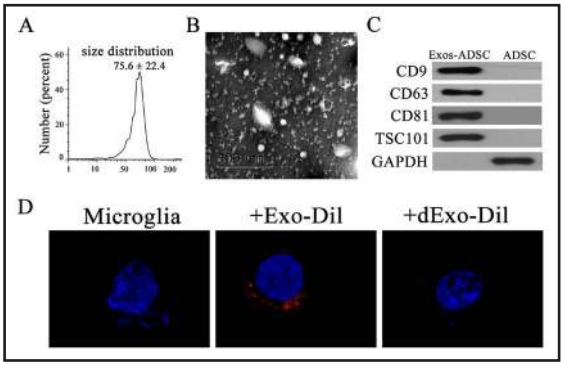

Fig. 3. Characterization of ADs-Exos. (A) Particle size distribution measured by DLS. (B) Morphology observed by TEM. Scale bar: 500 nm. (C) Expression of the exosome markers CD9, CD63, CD81, TSC101, and GAPDH confirmed by immunoblotting. Exosome lysate was loaded into the left lane and cell lysate into the right. (D) Representative micrographs of primary microglia or primary microglia incubated with DiI-labelled Exos (+Exo-DiI) or with DiI-labelled EVs denatured by boiling (+dExo-DiI).

promote the inflammatory response by suppressing M2 macrophage polarization [33-35]. Consequently, we aimed to identify whether Exos from ADSCs have a therapeutic effect on the OGD-induced inflammatory response in primary microglia by promoting autophagy. Exosomes were purified from ADSCs which was isolated and positive for the mesenchymal stem cell (MSC) markers CD29, CD90, CD44, and CD105 and negative for the endothelial markers vWF (Fig. 2), and their size distribution was determined to be slightly below 100 nm by dynamic light scattering (Fig. 3A). Transmission electron microscopy was used to identify exosomes from the ADSC culture medium. Ultrastructural analysis of ADSC-derived exosomes confirmed that they have a diameter of around 100 nm (Fig. 3B). Expression of the exosome markers CD9, CD63, CD81 and TSG101 was then confirmed by western blotting (Fig. 3C). Fig. 2D shows representative micrographs of primary microglia containing positively-stained DiI-labelled exosomes and the absence of staining in primary microglia where exosomes have been denatured by boiling.

To compare the therapeutic effect between Exos and miR-30d-5p-Exos on ischemia-induced nerve injury, ADSCs were transfected with miR-30d-5p over-expression mimic, cultured for 48 h, and then harvested for RT-PCR analysis. The results showed that the expression of miR-30d-5p in both ADSCs and Exos was increased after transfection with miR-30d-5p mimic (Fig. 4A and 4B).

Primary microglia cells were treated with or without Exos (10 μg/mL) under OGD conditions for 6 h. Immunofluorescence images of cells double-stained with LC-3 (green) and Iba-1 (red) showed that LC3-puncta in primary microglia were increased after OGD induction compared with the control group. Exos treatment significantly suppressed the formation of autophagy plaques, especially in the miR-30d-5p-overexpressing Exos treatment group (Fig. 4C and 4D). Western blot detection further confirmed that treatment with Exos, especially miR-30d-5p-overexpressing Exos, reversed the OGD-induced promotion of expression of the autophagy-related proteins Beclin-1, Atg-5 and LC-3, but increased P62 expression (Fig. 4E–I). These findings suggest that the protective effect of Exos in ischemia-induced brain injury

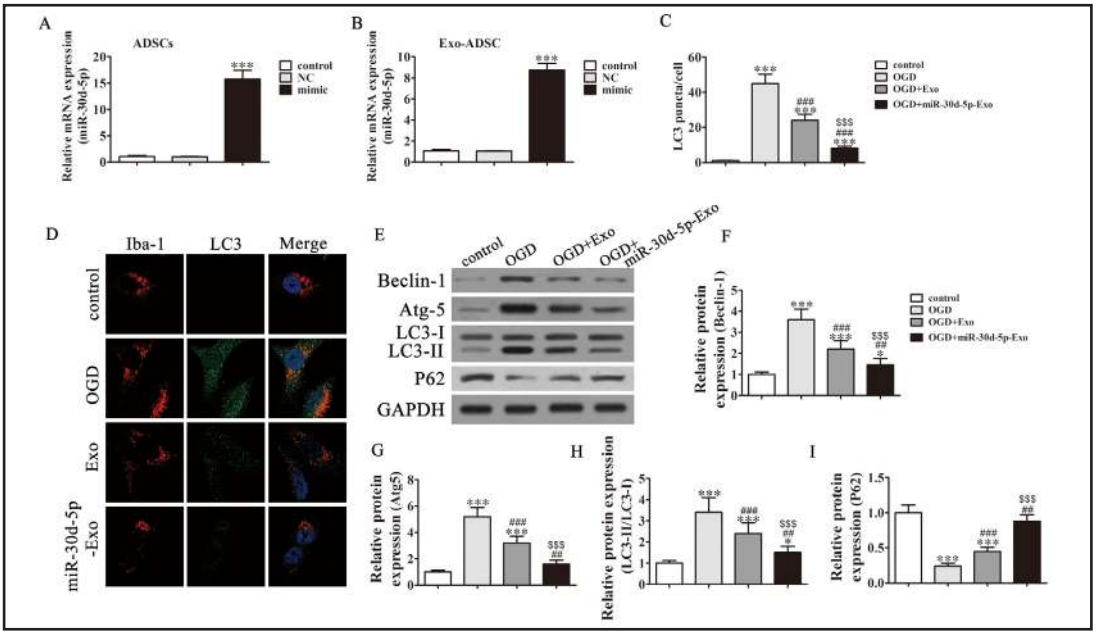

Fig. 4. Comparing the treatment effect of Exos from ADSCs or miR-30d-5p-overexpressing ADSCs on OGD-induced autophagy of primary microglia. Primary microglial cells were treated with or without Exos (10 μg/mL) under OGD conditions for 6 h. (A and B) RT-PCR analysis shows the expression of miR-30d-5p after transfection with miR-30d-5p mimic for 48 h in both ADSCs (A) and exosomes from ADSCs (B). Data are presented as mean ± SD. ***P<0.001 vs. control group. (C) Quantitative analysis of immunofluorescence of LC3-puncta in primary microglia double-stained with LC-3 and Iba-1. Data are presented as mean ± SD. ***P<0.001 vs. control group. $^{###}$P<0.001 vs. OGD group. $^{$$$}$P<0.001 vs. OGD+Exo group. (D) Representative immunofluorescence images of LC3-puncta in primary microglia double-stained with LC-3 (green) and Iba-1 (red). (E) Western blot showing the expression of the autophagy-related proteins LC3, P62, Beclin-1 and Atg5. GAPDH served as an internal control. (F–I) The relative protein levels were analyzed and data are represented as mean ± SD (n = 3). *P<0.05, ***P<0.001 vs. control group. $^{##}$P<0.01, $^{###}$P<0.001 vs. OGD group. $^{$$$}$P<0.001 vs. OGD+Exo group.

are related to autophagy inhibition, especially in treatment with miR-30d-5p-overexpressing Exos.

Treatment with miR-30d-5p-Exos is more effective in suppressing the inflammatory response by reversing OGD-induced and autophagy-mediated microglial polarization to M1.

To identify whether ischemia-induced brain injury is related to regulation of microglia activation and polarization, primary microglia cells were treated with/without Exos (10 μg/mL) or 3-Ma (2 mM) under OGD conditions for 6 h, then collected for immunofluorescence analysis. The results show that Exos treatment reversed OGD-induced M1 microglia/macrophage conversion, especially in the miR-30d-5p overexpressing Exos treatment group (Fig.. 5A and 5B), and promoted conversion of microglia into M2 microglia/macrophages (5C and 5D). Further, treatment with 3-Ma (an autophagy inhibitor) confirmed that the microglia/macrophage polarization was related to autophagy. Suppression of autophagy can promote OGD-induced polarization of microglia into M2 microglia/macrophages. ELISA detection showed that Exos treatment reversed increases in the expression of the inflammatory factors TNF-α, IL-6 and iNOS, which are markers secreted by M1 microglia/macrophages. However, Exos treatment increased expression of IL-4 and IL-10, the markers secreted by M2 microglia/macrophages (Fig. 5E–I). Treatment with Exos from miR-30d-5p-overexpressing ADSCs have a greater effect in suppressing inflammatory factor expression and promoting M2 microglial/macrophage conversion. These data suggest that the expression of miR-30d-

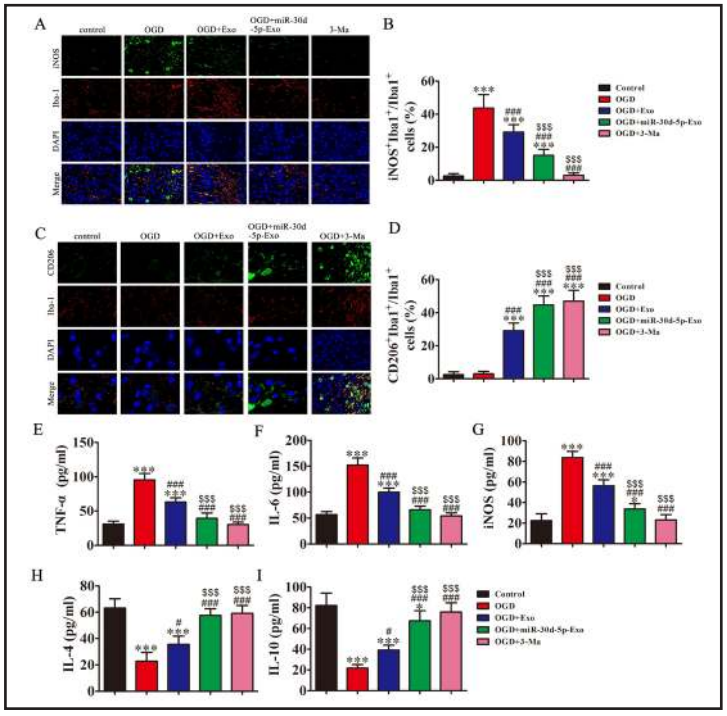

Fig. 5. miR-30d-5p-Exos treatment is more effective in suppressing the inflammatory response by reversing OGD-induced and autophagy-mediated microglia polarization to M1. Primary microglia cells were treatment with/without Exos (10 μg/mL) or 3-Ma (2 mM) under OGD condition for 6 h. (A) Representative images of double immunofluorescent staining of microglia with the microglia/macrophage marker, Iba1 (red), and the M1 marker, iNOS (green). (B) Quantification of the percentage of $iNOS^+/Iba\text{-}1^+$ cells among total Iba-1+ cells. Data are presented as mean ± SD (n = 10). $^{***}P<0.001$ vs. control group. $^{###}P<0.001$ vs. OGD group. $^{\$\$\$}P<0.001$ vs. OGD+Exo group. (C) Representative images of double immunofluorescent staining of microglia with the microglia/macrophage marker, Iba1 (red), and the M2 marker, CD206 (green). (D) Quantification of the percentage of $CD206^+/Iba\text{-}1^+$ cells among total Iba-1+ cells. Data are presented as mean ± SD (n = 10). $^{***}P<0.001$ vs. control group. $^{###}P<0.001$ vs. OGD group. $^{\$\$\$}P<0.001$ vs .OGD+Exo group. (E–I) Levels of the inflammatory cytokines TNF-α (E), IL-6 (F), iNOS (G), IL-4 (H) and IL-10 (I) in cellular supernatant were measured by ELISA. The relative protein levels were analyzed and data are presented as mean ± SD (n = 5). $^{*}P<0.05$, $^{***}P<0.001$ vs. control group. $^{\#}P<0.05$, $^{###}P<0.001$ vs. OGD group. $^{\$\$\$}P<0.001$ vs. OGD+Exo group.

5p has a greater effect in inhibiting autophagy. These results were confirmed with 3-Ma treatment.

Both Beclin-1 and Atg5 are direct targets of miR-30d-5p

Possible interactions between miR-30d-5p and Beclin-1 or Atg5 were predicted by bioinformatics analysis (http://www.targetscan.org/). Overlap analyses showed that miR-30d-5p had a broadly-conserved binding site (Fig. 6A). A mutated version of both the Beclin-1 and Atg5 3′-UTR was constructed in which six complementary nucleotides in the binding site were altered (Fig. 6B and 6C). This mutated construct was fused to the luciferase coding region (PYr-RGS-17 3′-UTR) and co-transfected into HEK293T cells along with miR-30d-5p mimic. The relative luciferase activity showed that when the wild-type Beclin-1 and Atg5 3′-UTR were co-transfected with miR-30d-5p mimic, expression of both Beclin-1 and Atg5 was significantly decreased ($P < 0.001$) compared with co-transfection with the control miRNA. However, this effect was not observed after transfection with the mutant 3′-UTR of Beclin-1 or Atg5, indicating that miR-30d-5p can specifically target and suppress the 3′-UTR of both Beclin-1 and Atg5 (Fig. 6D and 6E). Western blot analyses further confirmed that miR-30d-5p overexpression significantly inhibited expression of both Beclin-1 (Fig. 6F and 6G) and Atg5 (Fig. 6H and 6I) at the protein level *in vitro*. This suggests that miR-30d-5p-abundant Exos have a greater effect in suppressing autophagy.

Treatment with miR-30d-5p-Exos is more effective in ameliorating MCAO-induced brain injury

To identify the effects of Exos in ischemia-induced brain injury, stroke was induced in rats by MCAO, after which Exos were injected into the tail vein. At 3 h after stroke, brain

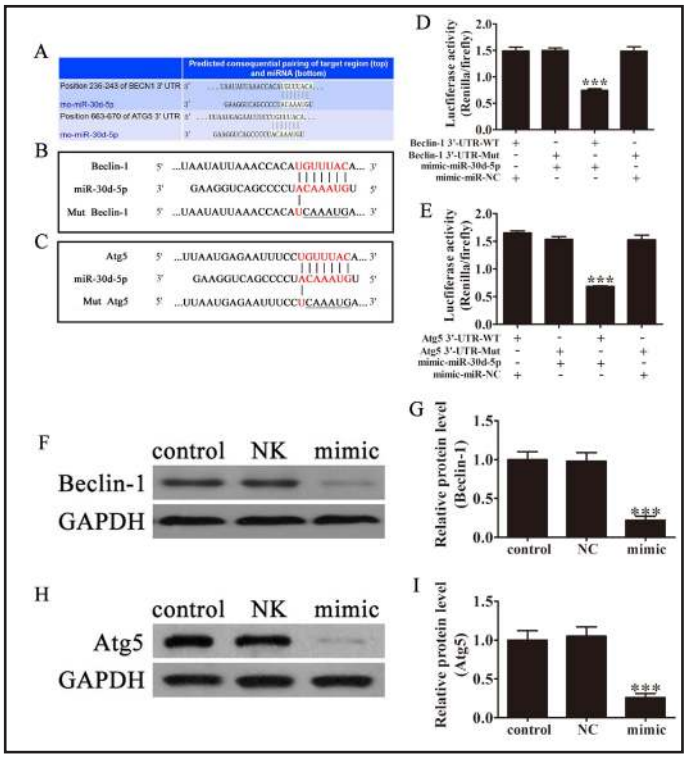

Fig. 6. Both Beclin-1 and Atg5 are potential targets of miR-30d-5p. (A) Complementary sequences between miR-30d-5p and the 3′-UTR of Beclin-1 and Atg5 mRNA were obtained using publicly-available algorithms. (B and C) The mutated versions of both the Beclin-1 (B) and Atg5 (C) 3′-UTR are also shown. The 3′-UTR of Beclin-1 and Atg5 were fused to the luciferase coding region (PYr-RGS-17 3′-UTR) and co-transfected into HEK293T cells with miR-30d-5p mimic to confirm that Beclin-1 and Atg5 are targets of miR-30d-5p. (D and E) The PYr-RGS-17 3′-UTR and miR-30d-5p mimic constructs were co-transfected into HEK293T cells with a control vector and the relative luciferase activity was determined 48 h after transfection. The data are expressed as the mean ± SD. ***P<0.001 vs. the control. (F–I) Western blot analysis of the effect of Beclin-1 (F and G) and Atg5 (H and I) expression in microglia cells after transfection with miR-30d-5p mimics (n = 5). GAPDH expression levels were detected as an endogenous control. All data are expressed as the mean ± SD. ***P<0.001 vs. control.

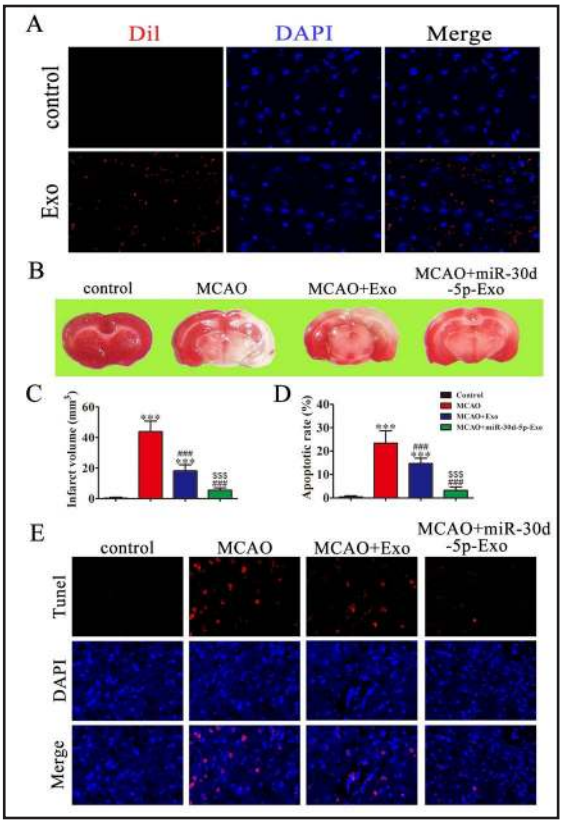

Fig. 7. miR-30d-5p-Exos treatment is more effective in suppressing MCAO-induced brain injury. Stroke was induced in rats by permanent occlusion of the MCAO. Exosomes were injected via the tail vein after induction of ischemia. Three hours or three days after stroke, brain coronal sections were harvested. (A) Representative immunofluorescence images of ischemic regions from rats receiving Exos 3 h after tail vein injection. (B) Representative TTC staining 3 days after MCAO. (C) Infarct volume in MCAO rats with or without exosome treatment were measured. The data are presented as mean ± SD (n = 6). ***P<0.001 vs. control group. ###P<0.001 vs. MCAO group. $$$P<0.001 vs. MCAO+Exo group. (D) The quantification of NeuN and TUNEL double-labeled cells. Data are presented as mean ± SD (n = 10). ***P<0.001 vs. control group. ###P<0.001 vs. MCAO group. $$$P<0.001 vs. MCAO+Exo group. (E) Representative images of NeuN- and TUNEL-staining 3 days after MCAO with or without exosome treatment.

coronal sections were harvested. Immunofluorescence images of the ischemic region show that Exos localize to the ischemic area (Fig. 7A). Three days after stroke, M1/M2 microglia markers and infarct volume were measured using immunofluorescence and TTC staining, respectively. TTC staining showed that infarct volumes were significantly larger in the MCAO group compared with controls, but that Exos treatment significantly decreased MCAO-induced infarct volume, especially in the miR-30d-5p-overexpression group (Fig. 7B and 7C). Immunohistochemistry was used to detect apoptosis of nerve cells at 3 days after stroke (Fig. 7D and 7E). The assay results confirmed that Exos treatment reversed ischemia-induced neuronal apoptosis, especially in the miR-30d-5p overexpression group.

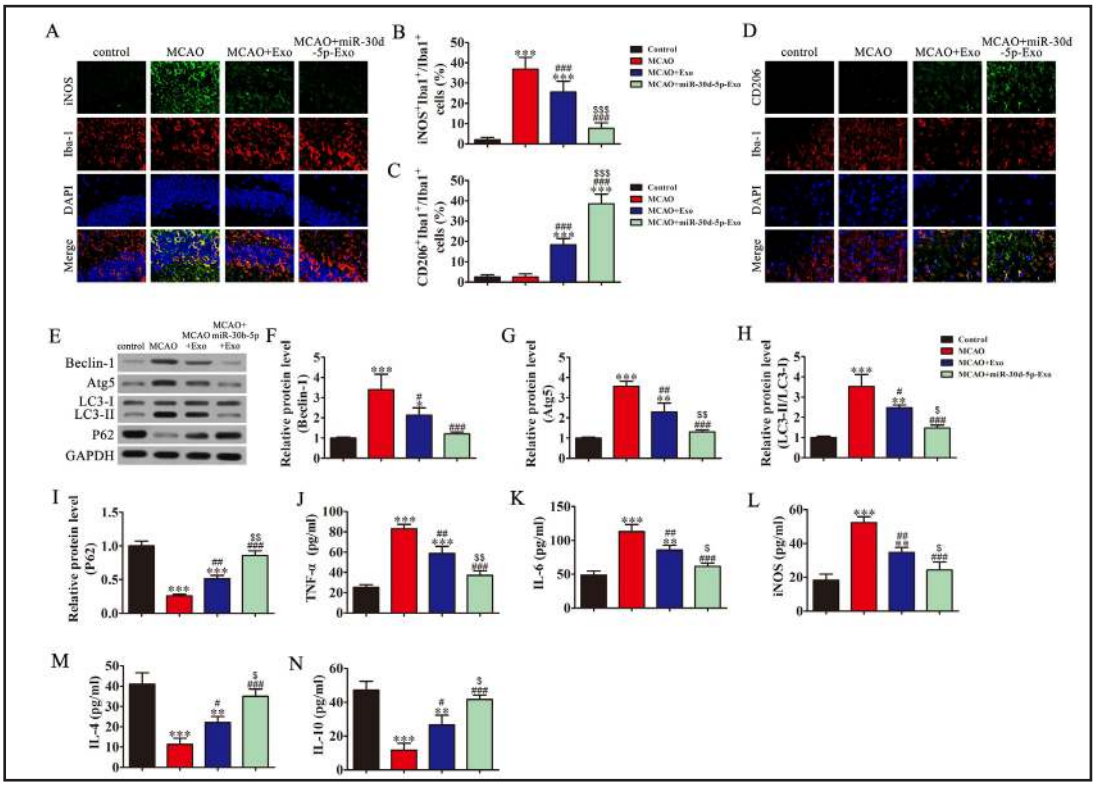

Fig. 8. miR-30d-5p-Exos treatment inhibits the autophagy-mediated inflammatory response by promoting microglia polarization to M2 after MCAO. (A and B) Representative images of double immunofluorescent staining in the ischemic cortex with the microglia/macrophage marker, Iba1 (red), and the M1 marker, iNOS (green). Quantification of the percentage of $iNOS^+/Iba\text{-}1^+$ cells among total Iba-1+ cells. Data are presented as mean ± SD (n = 10). $^{***}P<0.001$ vs. control group. $^{###}P<0.001$ vs. MCAO group. $^{\$\$\$}P<0.001$ vs. MCAO+Exo group. (C) Quantification of the percentage of $CD206^+/Iba\text{-}1^+$ cells among total Iba-1+ cells. Data are presented as mean ± SD (n = 6). $^{***}P<0.001$ vs. control group. $^{###}P<0.001$ vs. MCAO group. $^{\$\$\$}P<0.001$ vs. MCAO+Exo group. (D) Representative images of double immunofluorescent staining in the ischemic cortex with the microglia/macrophage marker, Iba1 (red), and the M2 marker, CD206 (green). (E) Western blot showing the expression of the autophagy-related proteins LC3, P62, Beclin-1 and Atg5 in brain tissues. GAPDH served as an internal control. (F–I) The relative protein levels were analyzed and data are represented as mean ± SD (n = 3). Data are presented as mean ± SD (n = 6). $^{*}P<0.05$, $^{**}P<0.01$, $^{***}P<0.001$ vs. control group. $^{\#}P<0.05$, $^{\#\#}P<0.01$, $^{\#\#\#}P<0.001$ vs. MCAO group. $^{\$}P<0.05$, $^{\$\$}P<0.01$ vs. MCAO+Exo group. (J–N) Levels of the inflammatory cytokines TNF-α (J), IL-6 (K), iNOS (L), IL-4 (M) and IL-10 (N) in brain tissues were measured by ELISA. The relative protein levels were analyzed and data are presented as mean ± SD (n = 10). $^{**}P<0.01$, $^{***}P<0.001$ vs. control group. $^{\#}P<0.05$, $^{\#\#}P<0.01$, $^{\#\#\#}P<0.001$ vs. MCAO group. $^{\$}P<0.05$, $^{\$\$}P<0.01$ vs. MCAO+Exo group.

miR-30d-5p-Exos treatment inhibits the autophagy-mediated inflammatory response by promoting microglia polarization to M2 after MCAO.

Immunofluorescence illuminated the effects of Exos on microglia/macrophage phenotypic responses in mice 3 days after stroke. Exos treatment reduced expression of the M1 marker, iNOS (Fig. 8A and 8B), and increased expression of the M2 marker, CD206 (Fig. 8C and 8D). Treatment with miR-30d-5p-overexpressing Exos had the best effect in promoting polarization of microglia into M2. Exos treatment also reversed the MCAO-induced expression of autophagy-related proteins Beclin-1, Atg5, and LC3 in brain tissue (Fig. 8E–I). ELISA showed that Exos treatment decreased expression of TNF-α, IL-6 and iNOS, but increased IL-4 and IL-10 levels (Fig. 8J–N).

Discussion

In this study, we have investigated whether ADSC-derived exosomes enriched with microRNA (miR)-30d-5p have a protective effect on AIS by examining their effect on cells from subjects with AIS and on an ischemic model *in vivo* and *in vitro*. Our main findings were as follows: (i) expression of the inflammatory cytokines TNF-α, IL-6 and iNOS are induced, while the anti-inflammatory cytokines IL-4, IL-10 and miR-30d-5p are reduced following AIS in both patients and animal models; (ii) *in vitro* studies demonstrate that suppression of autophagy significantly reduces the OGD-induced inflammatory response. In addition, exosome treatment is more effective in suppressing the inflammatory response by reversing the OGD-induced and autophagy-mediated microglial polarization to M1, and (iii) *in vivo* studies show that exosomes derived from ADSCs significantly decrease the cerebral injury area of infarction by suppressing autophagy and promoting M2 microglia/macrophage polarization.

Recent evidence suggests that microglia cells play an active role in normal brain function, and the importance of active neuronal–microglial interaction in the maintenance of homeostasis in the extracellular microenvironment has become increasingly appreciated [27]. The functions of microglia become more significant in response to a CNS insult such as ischemia. Increasing evidence suggests that an increase in the brain M2/M1 ratio and increases of M2 microglial proteins have anti-inflammatory properties and provide a neuroprotective effect [36, 37]. IL-4 and IL-10 are markers secreted by M2 microglial cells, while TNF-α, IL-6 and iNOS are markers secreted by M1 microglial cells [38-41]. suggesting that M1 microglia are increased in AIS patients. We also found that the expression of miR-30d-5p was decreased, which is related to autophagy regulation, while autophagy is related to the inflammatory response [42, 43]. The results show that miR-30d-5p can significantly suppress ischemia-induced autophagy by targeting both Beclin-1 and Atg5. Ultimately it suppresses ischemia-induced and autophagy-mediated microglial polarization to M1. Together, these data indicate that overexpression of miR-30d-5p may have an important regulatory role in neuroprotection.

Emerging data show that exosomes released from MSCs have therapeutic benefits in stroke. MSC-derived exosomes are capable of transferring miR-133b to neurons and subsequently contribute to neurite outgrowth after stroke [44, 45]. These data indicate that MSC-derived exosomes not only cross the blood–brain barrier (BBB), but also deliver functional cargo to modulate gene expression in the recipient cells. Due to their small size, exosomes can avoid phagocytosis by macrophages. They are naturally able to evade endosomal-lysosomal degradation, in contrast to polymeric nanoparticles and liposomes. Combined with their lack of immunogenicity, these features make exosomes promising candidates for gene drug delivery [46]. In our study, we found that exosomes from miR-30d-5p-overexpressing ADSCs suppressed ischemia-induced neuronal damage by inhibiting the autophagy-mediated inflammatory response in *in vivo* and *in vitro* experiments. Our results also found that the expression of miR-30d-5p can significantly inhibit both Beclin-1 and Atg5 expression by targeting the 3'UTR of Beclin-1 and Atg5 at the mRNA level. Suppression

of autophagy can transform microglial/macrophage polarization from M1 to M2 under ischemic conditions. These findings suggest that the protective effect of Exos in AIS-induced brain injury depends on regulation of autophagy and microglial/macrophage polarization. Exosome-mediated delivery of miR-30d-5p suppresses autophagy-mediated brain injury by promoting M2 microglial/macrophage polarization.

Conclusion

In summary, our results show that exosomes are efficient tools for gene drug delivery to the ischemic cortex. In addition, exosomes loaded with miR-30d-5p can reverse ischemia-induced, autophagy-mediated brain injury by promoting M2 microglial/macrophage polarization. Our study suggests that treatment with exosomes from miR-30d-5p-overexpressing ADSCs during the acute phase of stroke could be a promising therapeutic strategy for ameliorating cerebral injury by inhibiting the inflammatory response.

Acknowledgements

This study was supported by The Foundation of Discipline Leader in Health Systems of Pudong New District (No. PWRd2014-09 for Mei Jiang, PWRd2014-02 for Limin Xu, PWRd2011-04 for Hairong Wang); Science and Technology Development Fund of Pudong New District Minsheng Scientific Research (Medical and Health) Project (No. PKJ2017-Y24 for Mei Jiang); the National Natural Science Foundation of China (No. 81201029 for Mei Jiang); the Key Specialty Construction Project of Shanghai Municipal Commission of Health and Family Planning (No. ZK2015B16) and a Municipal Human Resources Development Program for Outstanding Leaders in Medical Disciplines in Shanghai (No. 2017BR051).

MJ, HW, LX, LL and QD designed the studies and prepared the manuscript with comments from all authors. XY, HX, HZ and FW performed all the experiments and analyzed the data. XL, GW, RH, LC and XG carried out in all experiments and revised the manuscript.

Disclosure Statement

The authors declare that there is no conflict of interests regarding the publication of this paper.

References

1 Lloyd-Jones D, Adams R, Carnethon M, De Simone G, Ferguson TB, Flegal K, Ford E, Furie K, Go A, Greenlund K, Haase N, Hailpern S, Ho M, Howard V, Kissela B, Kittner S, Lackland D, Lisabeth L, Marelli A, McDermott M, Meigs J, Mozaffarian D, Nichol G, O'Donnell C, Roger V, Rosamond W, Sacco R, Sorlie P, Stafford R, Steinberger J, Thom T, Wasserthiel-Smoller S, Wong N, Wylie-Rosett J, Hong Y: Heart disease and stroke statistics--2009 update: A report from the american heart association statistics committee and stroke statistics subcommittee. Circulation 2009;119:480-486.

2 Lackland DT, Roccella EJ, Deutsch AF, Fornage M, George MG, Howard G, Kissela BM, Kittner SJ, Lichtman JH, Lisabeth LD, Schwamm LH, Smith EE, Towfighi A: Factors influencing the decline in stroke mortality: A statement from the american heart association/american stroke association. Stroke 2014;45:315-353.

3 Cai J, Xu D, Bai X, Pan R, Wang B, Sun S, Chen R, Sun J, Huang Y: Curcumin mitigates cerebral vasospasm and early brain injury following subarachnoid hemorrhage via inhibiting cerebral inflammation. Brain Behav 2017;7:e00790.

4 Ghosh M, Xu Y, Pearse DD: Cyclic amp is a key regulator of m1 to m2a phenotypic conversion of microglia in the presence of th2 cytokines. J Neuroinflammation 2016;13:9.

5 Ansari MA: Temporal profile of m1 and m2 responses in the hippocampus following early 24h of neurotrauma. J Neurol Sci 2015;357:41-49.
6 Schmieder A, Michel J, Schonhaar K, Goerdt S, Schledzewski K: Differentiation and gene expression profile of tumor-associated macrophages. Semin Cancer Biol 2012;22:289-297.
7 Brifault C, Gras M, Liot D, May V, Vaudry D, Wurtz O: Delayed pituitary adenylate cyclase-activating polypeptide delivery after brain stroke improves functional recovery by inducing m2 microglia/ macrophage polarization. Stroke 2015;46:520-528.
8 Xie Z, Klionsky DJ: Autophagosome formation: Core machinery and adaptations. Nat Cell Biol 2007;9:1102-1109.
9 Shintani T, Klionsky DJ: Autophagy in health and disease: A double-edged sword. Science 2004;306:990-995.
10 Mizushima N, Komatsu M: Autophagy: Renovation of cells and tissues. Cell 2011;147:728-741.
11 Levine B, Kroemer G: Autophagy in the pathogenesis of disease. Cell 2008;132:27-42.
12 Liu XS, Chopp M, Zhang RL, Zhang ZG: Micrornas in cerebral ischemia-induced neurogenesis. J Neuropathol Exp Neurol 2013;72:718-722.
13 Mirzaei H: Stroke in women: Risk factors and clinical biomarkers. J Cell Biochem 2017;118:4191-4202.
14 Dharap A, Bowen K, Place R, Li LC, Vemuganti R: Transient focal ischemia induces extensive temporal changes in rat cerebral microrna ome. J Cereb Blood Flow Metab 2009;29:675-687.
15 Jeyaseelan K, Lim KY, Armugam A: Microrna expression in the blood and brain of rats subjected to transient focal ischemia by middle cerebral artery occlusion. Stroke 2008;39:959-966.
16 Mirzaei H, Momeni F, Saadatpour L, Sahebkar A, Goodarzi M, Masoudifar A, Kouhpayeh S, Salehi H, Mirzaei HR, Jaafari MR: Microrna: Relevance to stroke diagnosis, prognosis, and therapy. J Cell Physiol 2018;233:856-865.
17 Luo Q, Guo D, Liu G, Chen G, Hang M, Jin M: Exosomes from mir-126-overexpressing adscs are therapeutic in relieving acute myocardial ischaemic injury. Cell Physiol Biochem 2017;44:2105-2116.
18 Zhao F, Qu Y, Zhu J, Zhang L, Huang L, Liu H, Li S, Mu D: Mir-30d-5p plays an important role in autophagy and apoptosis in developing rat brains after hypoxic-ischemic injury. J Neuropathol Exp Neurol 2017;76:709-719.
19 Lam PK, Chong CCN, Lo AWI, Chan AWH, Tong CSW, Chin DWC, Wong KHK, Choy RKW, Fung AK, Wang YX, To KF, Lai PBS: Topical application of mesenchymal stromal cells ameliorated liver parenchyma damage after ischemia-reperfusion injury in an animal model. Transplant Direct 2017;3:e160.
20 Zhang H, Sun F, Wang J, Xie L, Yang C, Pan M, Shao B, Yang GY, Yang SH, ZhuGe Q, Jin K: Combining injectable plasma scaffold with mesenchymal stem/stromal cells for repairing infarct cavity after ischemic stroke. Aging Dis 2017;8:203-214.
21 He J, Wang Y, Sun S, Yu M, Wang C, Pei X, Zhu B, Wu J, Zhao W: Bone marrow stem cells-derived microvesicles protect against renal injury in the mouse remnant kidney model. Nephrology (Carlton) 2012;17:493-500.
22 Du Y, Li D, Han C, Wu H, Xu L, Zhang M, Zhang J, Chen X: Exosomes from human-induced pluripotent stem cell-derived mesenchymal stromal cells (hipsc-mscs) protect liver against hepatic ischemia/ reperfusion injury via activating sphingosine kinase and sphingosine-1-phosphate signaling pathway. Cell Physiol Biochem 2017;43:611-625.
23 Liu L, Jin X, Hu CF, Li R, Zhou Z, Shen CX: Exosomes derived from mesenchymal stem cells rescue myocardial ischaemia/reperfusion injury by inducing cardiomyocyte autophagy via ampk and akt pathways. Cell Physiol Biochem 2017;43:52-68.
24 Hatano S: Experience from a multicentre stroke register: A preliminary report. Bull World Health Organ 1976;54:541-553.
25 Xu C, Liu J, Chen L, Liang S, Fujii N, Tamamura H, Xiong H: Hiv-1 gp120 enhances outward potassium current via cxcr4 and camp-dependent protein kinase a signaling in cultured rat microglia. Glia 2011;59:997-1007.
26 Yang J, Zhang X, Chen X, Wang L, Yang G: Exosome mediated delivery of mir-124 promotes neurogenesis after ischemia. Mol Ther Nucleic Acids 2017;7:278-287.
27 Qin AP, Liu CF, Qin YY, Hong LZ, Xu M, Yang L, Liu J, Qin ZH, Zhang HL: Autophagy was activated in injured astrocytes and mildly decreased cell survival following glucose and oxygen deprivation and focal cerebral ischemia. Autophagy 2010;6:738-753.

28 Teng X, Chen L, Chen W, Yang J, Yang Z, Shen Z: Mesenchymal stem cell-derived exosomes improve the microenvironment of infarcted myocardium contributing to angiogenesis and anti-inflammation. Cell Physiol Biochem 2015;37:2415-2424.
29 Caserta S, Kern F, Cohen J, Drage S, Newbury SF, Llewelyn MJ: Circulating plasma microrna can differentiate human sepsis and systemic inflammatory response syndrome (sirs). Sci Rep 2016;6:28006.
30 Subramanian S, Pallati PK, Sharma P, Agrawal DK, Nandipati KC: Trem-1 associated macrophage polarization plays a significant role in inducing insulin resistance in obese population. J Transl Med 2017;15:85.
31 Shao BZ, Ke P, Xu ZQ, Wei W, Cheng MH, Han BZ, Chen XW, Su DF, Liu C: Autophagy plays an important role in anti-inflammatory mechanisms stimulated by alpha7 nicotinic acetylcholine receptor. Front Immunol 2017;8:553.
32 Ko JH, Yoon SO, Lee HJ, Oh JY: Rapamycin regulates macrophage activation by inhibiting nlrp3 inflammasome-p38 mapk-nfkappab pathways in autophagy- and p62-dependent manners. Oncotarget 2017;8:40817-40831.
33 Shan M, Qin J, Jin F, Han X, Guan H, Li X, Zhang J, Zhang H, Wang Y: Autophagy suppresses isoprenaline-induced m2 macrophage polarization via the ros/erk and mtor signaling pathway. Free Radic Biol Med 2017;110:432-443.
34 Luo J, Hu YL, Wang H: Ursolic acid inhibits breast cancer growth by inhibiting proliferation, inducing autophagy and apoptosis, and suppressing inflammatory responses via the pi3k/akt and nf-kappab signaling pathways *in vitro*. Exp Ther Med 2017;14:3623-3631.
35 Xu XC, Wu YF, Zhou JS, Chen HP, Wang Y, Li ZY, Zhao Y, Shen HH, Chen ZH: Autophagy inhibitors suppress environmental particulate matter-induced airway inflammation. Toxicol Lett 2017;280:206-212.
36 Kumar A, Barrett JP, Alvarez-Croda DM, Stoica BA, Faden AI, Loane DJ: Nox2 drives m1-like microglial/macrophage activation and neurodegeneration following experimental traumatic brain injury. Brain Behav Immun 2016;58:291-309.
37 Gao J, Grill RJ, Dunn TJ, Bedi S, Labastida JA, Hetz RA, Xue H, Thonhoff JR, DeWitt DS, Prough DS, Cox CS, Jr., Wu P: Human neural stem cell transplantation-mediated alteration of microglial/macrophage phenotypes after traumatic brain injury. Cell Transplant 2016;25:1863-1877.
38 Hao J, Hu Y, Li Y, Zhou Q, Lv X: Involvement of jnk signaling in il4-induced m2 macrophage polarization. Exp Cell Res 2017;357:155-162.
39 Lurier EB, Dalton D, Dampier W, Raman P, Nassiri S, Ferraro NM, Rajagopalan R, Sarmady M, Spiller KL: Transcriptome analysis of il-10-stimulated (m2c) macrophages by next-generation sequencing. Immunobiology 2017;222:847-856.
40 Tian L, Li W, Yang L, Chang N, Fan X, Ji X, Xie J, Li L: Cannabinoid receptor 1 participates in liver inflammation by promoting m1 macrophage polarization via rhoa/nf-kappab p65 and erk1/2 pathways, respectively, in mouse liver fibrogenesis. Front Immunol 2017;8:1214.
41 Cheng Y, Feng Y, Xia Z, Li X, Rong J: Omega-alkynyl arachidonic acid promotes anti-inflammatory macrophage m2 polarization against acute myocardial infarction via regulating the cross-talk between pkm2, hif-1alpha and inos. Biochim Biophys Acta 2017;1862:1595-1605.
42 Li N, Tang B, Jia YP, Zhu P, Zhuang Y, Fang Y, Li Q, Wang K, Zhang WJ, Guo G, Wang TJ, Feng YJ, Qiao B, Mao XH, Zou QM: Helicobacter pylori caga protein negatively regulates autophagy and promotes inflammatory response via c-met-pi3k/akt-mtor signaling pathway. Front Cell Infect Microbiol 2017;7:417.
43 Han F, Xiao QQ, Peng S, Che XY, Jiang LS, Shao Q, He B: Atorvastatin ameliorates lps-induced inflammatory response by autophagy via akt/mtor signaling pathway. J Cell Biochem 2017
44 Xin H, Li Y, Liu Z, Wang X, Shang X, Cui Y, Zhang ZG, Chopp M: Mir-133b promotes neural plasticity and functional recovery after treatment of stroke with multipotent mesenchymal stromal cells in rats via transfer of exosome-enriched extracellular particles. Stem Cells 2013;31:2737-2746.
45 Xin H, Li Y, Buller B, Katakowski M, Zhang Y, Wang X, Shang X, Zhang ZG, Chopp M: Exosome-mediated transfer of mir-133b from multipotent mesenchymal stromal cells to neural cells contributes to neurite outgrowth. Stem Cells 2012;30:1556-1564.
46 Ha D, Yang N, Nadithe V: Exosomes as therapeutic drug carriers and delivery vehicles across biological membranes: Current perspectives and future challenges. Acta Pharm Sin B 2016;6:287-296.